Contemporary Avian Influenza A Virus Subtype H1, H6, H7, H10, and H15 Hemagglutinin Genes Encode a Mammalian Virulence Factor Similar to the 1918 Pandemic Virus H1 Hemagglutinin

Li Qi,[a] Lindsey M. Pujanauski,[a] A. Sally Davis,[a] Louis M. Schwartzman,[a] Daniel S. Chertow,[a,b] David Baxter,[c] Kelsey Scherler,[c] Kevan L. Hartshorn,[d] Richard D. Slemons,[e] Kathie-Anne Walters,[c] John C. Kash,[a] Jeffery K. Taubenberger[a]

Viral Pathogenesis and Evolution Section, Laboratory of Infectious Diseases, National Institute of Allergy and Infectious Diseases,[a] and Critical Care Medicine Department, Clinical Center,[b] National Institutes of Health, Bethesda, Maryland, USA; Institute for Systems Biology, Seattle, Washington, USA[c]; Department of Medicine, Boston University School of Medicine, Boston, Massachusetts, USA[d]; Department of Veterinary Preventive Medicine, Ohio State University, Columbus, Ohio, USA[e]

ABSTRACT Zoonotic avian influenza virus infections may lead to epidemics or pandemics. The 1918 pandemic influenza virus has an avian influenza virus-like genome, and its H1 hemagglutinin was identified as a key mammalian virulence factor. A chimeric 1918 virus expressing a contemporary avian H1 hemagglutinin, however, displayed murine pathogenicity indistinguishable from that of the 1918 virus. Here, isogenic chimeric avian influenza viruses were constructed on an avian influenza virus backbone, differing only by hemagglutinin subtype expressed. Viruses expressing the avian H1, H6, H7, H10, and H15 subtypes were pathogenic in mice and cytopathic in normal human bronchial epithelial cells, in contrast to H2-, H3-, H5-, H9-, H11-, H13-, H14-, and H16-expressing viruses. Mouse pathogenicity was associated with pulmonary macrophage and neutrophil recruitment. These data suggest that avian influenza virus hemagglutinins H1, H6, H7, H10, and H15 contain inherent mammalian virulence factors and likely share a key virulence property of the 1918 virus. Consequently, zoonotic infections with avian influenza viruses bearing one of these hemagglutinins may cause enhanced disease in mammals.

IMPORTANCE Influenza viruses from birds can cause outbreaks in humans and may contribute to the development of pandemics. The 1918 pandemic influenza virus has an avian influenza virus-like genome, and its main surface protein, an H1 subtype hemagglutinin, was identified as a key mammalian virulence factor. In a previous study, a 1918 virus expressing an avian H1 gene was as virulent in mice as the reconstructed 1918 virus. Here, a set of avian influenza viruses was constructed, differing only by hemagglutinin subtype. Viruses with the avian H1, H6, H7, H10, and H15 subtypes caused severe disease in mice and damaged human lung cells. Consequently, infections with avian influenza viruses bearing one of these hemagglutinins may cause enhanced disease in mammals, and therefore surveillance for human infections with these subtypes may be important in controlling future outbreaks.

Influenza A viruses continue to pose major challenges to public health, causing annual (seasonal) influenza epidemics in humans, emerging epizootics in domestic animals, zoonotic outbreaks at the human-animal interfaces, and the occasional and unpredictable emergence of human pandemic viruses with antigenically novel hemagglutinin (HA) subtypes (1). Although such viruses are able to infect many warm-blooded avian and mammalian species, the major reservoir is thought to be wild, free-ranging waterfowl and shorebirds (2). Eighteen distinct HA subtypes distinguished by high genetic and antigenic variability have been identified, 16 of which (subtypes H1 to H16) are consistently found in multiple avian host species (3, 4), but only 4 of these 16 have been incorporated within stably mammal-adapted influenza virus lineages—H1, H2, and H3 in humans, H1 and H3 in swine, H7 and H3 in equines, and H3 in canines (5).

The genetic pool of avian-origin influenza A (AI) viruses, containing 16 HA and 9 neuraminidase (NA) subtypes, is thus a major genomic source for novel viruses that can potentially adapt to domestic mammals and humans during stable host switch events (6). Novel host-switched viruses can adapt *in toto* or by genomic segment reassortment with other human- or mammal-adapted influenza A viruses (1). Since the appearance of highly pathogenic avian influenza (HPAI) H5N1 viruses causing infections in humans and more recently infections with low-pathogenicity avian influenza (LPAI) H7N9 and H10N8 viruses in humans, there has been heightened concern that AI viruses capable of causing hu-

man infections may lead to epidemics or pandemics (7). HPAI virus subtypes H5N1, H7N3, and H7N7 and LPAI viruses, including H9N2, H7N9, H6N1, H10N8, H7N2, and H7N3, have all caused human infections with variable morbidity and mortality (7–12). The mechanisms by which these avian viruses can stably adapt to mammals and to humans in particular remain poorly understood, as are the underlying determinants of severe pathogenicity in humans (9).

The 1918 H1N1 influenza pandemic resulted in approximately 50 million deaths worldwide (13), and while its origin is not fully elucidated, the virus is avian-like in both its coding sequences (5, 14, 15) and genome content (16, 17). The reconstructed 1918 virus has been used in a number of studies of host adaptation and pathogenicity (18, 19), and chimeric viruses expressing 1918 HA on contemporary human seasonal influenza virus genomic backgrounds have shown conclusively that the 1918 HA genomic segment encodes a key virulence factor for mammals (15, 20–23). Similar to observations in 1918-1919 human autopsy studies (24), the fully reconstructed 1918 virus causes extensive viral pneumonia in mice, ferrets, and macaques, including a characteristic alveolitis with a prominent airspace neutrophil and macrophage infiltrate (23, 25–27). Chimeric viruses expressing 1918 HA on a background of seven other gene segments derived from a contemporary human seasonal H1N1 virus also induced a similar respiratory tract pathology, with prominent alveolar neutrophils and macrophages (22), indicating that the pathogenicity of the 1918 virus is substantially derived from its H1 HA.

In a recent study, a set of eight chimeric "7:1" 1918 viruses was constructed by replacing one gene segment at a time from a contemporary "prototypic" LPAI H1N1 virus (15). The LPAI virus induced neither weight loss nor pathogenic changes, while the fully reconstructed 1918 virus induced a lethal infection. However, the 1918 chimeric virus encoding avian PB2 was attenuated in mice, and this attenuation was corrected by a single coding mutation, E627K (15). This mutation previously was shown to be associated with host restriction (28, 29) and with enhanced replication in mice (30–32). In light of the fact that the 1918 virus H1 is known to be a major virulence factor, the most unexpected observation was that the chimeric 1918 virus encoding the avian H1 HA was not attenuated compared to the fully reconstructed 1918 virus in mice but rather induced a severe respiratory pathology indistinguishable from that of the parental 1918 virus (15).
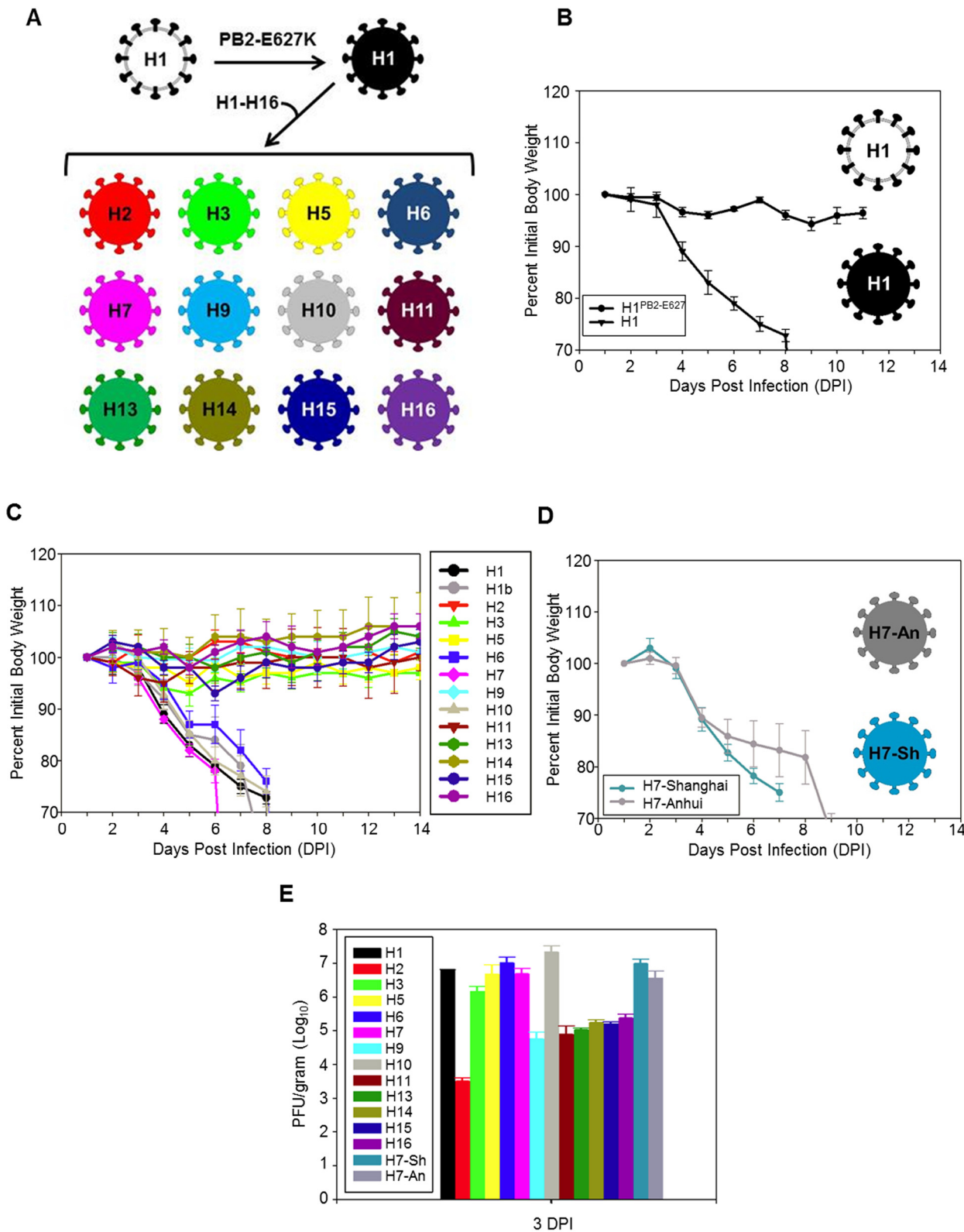
These observations led to the hypothesis that the mammalian virulence associated with the 1918 H1 HA was not unique to the pandemic HA but was apparently shared with a contemporary LPAI virus H1 HA. Using the LPAI H1N1 PB2^{E627K} virus, containing a mutation which facilitates viral replication in mammalian cells (15), we compared pathogenicity and virulence properties of this virus in mice to those of a set of chimeric viruses expressing 13 different contemporary LPAI viral HA subtypes (H1 to -3, H5 to -7, H9 to -11, and H13 to -16) and included H7 genes from two recent human H7N9 zoonotic infection isolates (33). The chimeric AI viruses were isogenic for seven of their eight gene segments, differing only in the HA gene. These studies showed that chimeric AI viruses containing the H1, H6, H7, H10, and H15 HA subtypes were pathogenic in mice and cytopathic in human cells, providing evidence that zoonotic infections with avian influenza viruses expressing one of these five HA subtypes have the potential to cause more severe disease in mammals and possibly humans.

RESULTS

Mouse pathogenicity of isogenic influenza viruses with different low-pathogenicity avian influenza virus HA subtypes. In a previous study, an H1N1 LPAI virus (termed here H1$^{PB2-E627}$) was evaluated in a comparative pathogenicity study along with the 1918 influenza virus and chimeric 7:1 1918:AI viruses in mice in which each of the eight chimeric viruses contained seven 1918 gene segments and one of the LPAI virus gene segments. Infection with the H1$^{PB2-E627}$ virus did not cause weight loss or induce pathological changes (15). In the current study, the PB2 gene of this H1N1 LPAI virus was altered with an E627K mutation to facilitate replication in mammalian cells, and this virus, here termed H1 (Fig. 1A), was evaluated for pathogenicity in mice (Fig. 1B). The H1 virus was then compared with a set of chimeric viruses differing only in the HA gene (see Table S1 in the supplemental material for sources of HA genes). Thus, chimeric AI viruses expressing representative HAs of different HA subtypes were constructed on a viral genetic background identical to that of the H1 virus (see Fig. S1). In addition, chimeric AI viruses expressing the H7 HA from two recent human-origin H7N9 virus isolates were also constructed. With the exception of these human H7N9 isolates, none of the avian-origin IAV viruses contained HA receptor binding domain mutations associated with mammalian adaptation. Isogenic viruses expressing the H4, H8, and H12 HA subtypes could not be recovered (see Table S1). The rescued chimeric "HxN1" viruses (expressing HA subtypes H1 to H3, H5 to H7, H9 to H11, and H13 to H16), each with an identical N1 subtype NA gene and identical viral genetic background in the other seven genomic segments, all grew comparably in MDCK cells (average peak titer of 7 log$_{10}$ PFU) (Table 1). Throughout this report, these otherwise isogenic viruses will be referred to by the HA subtype they express (Fig. 1A).

Viral lung titers and mouse pathogenicity of the H1 virus construct were compared to those of the parental H1N1$^{PB2-E627}$ LPAI virus. As expected (15), using an intranasal dose of 10^3 PFU in 50 μl, the H1$^{PB2-E627}$ virus induced no pathological changes (Table 1). In contrast, 10^3 PFU of the H1 virus with the PB2 E627K change was markedly pathogenic in mice, causing rapid weight loss and 100% mortality by day 8 ($n = 5$ per group) (Fig. 1B). This H1 virus was subsequently determined to have a mouse 50% lethal dose (MLD$_{50}$) of 1.8 log$_{10}$ PFU (Table 1) ($n = 5$ per dose), comparable to the MLD$_{50}$ of the fully reconstructed 1918 virus (15). In order to exclude that this pathogenic phenotype reflected a strain-specific phenomenon with the HA gene of the H1 virus, a second chimeric H1 virus, expressing the HA from another randomly selected LPAI virus H1 strain (H1b) (see Table S1 in the supplemental material), was rescued. The two H1 HA proteins contained 12 coding differences (4; also data not shown). The second H1 virus (H1b) was equally pathogenic in mice, with an MLD$_{50}$ (Fig. 1C and Table 1) comparable to those of the H1 and 1918 viruses (15).

To examine mouse pathogenicity in isogenic viruses expressing LPAI viral HA subtypes other than H1, animals were intranasally inoculated with 10^3 PFU in 50 μl of otherwise isogenic viruses containing seven gene segments from the above H1 virus and HA genes derived from the different LPAI donor viruses (see Table S1 and Fig. S1 in the supplemental material; $n = 5$ per group). A subset of these isogenic viruses induced rapid weight loss and fatal

FIG 1 Evaluation of chimeric avian influenza virus pathogenicity in mice. (A) Diagrammatic representation of the construction of the chimeric avian influenza A viruses utilized in the study (see Fig. S1 in the supplemental material and Materials and Methods for additional details). (B) Weight loss in mice following intranasal inoculation of 10^3 PFU of the $H1^{PB2-E627}$ and H1 viruses. (C) Weight loss in mice following intranasal inoculation of 10^3 PFU of the chimeric H1 to H16 viruses in mice. (D) Weight loss in mice following intranasal inoculation of 10^3 PFU of the H7-Shanghai and H7-Anhui viruses. (E) Lung titers (PFU/g) from the above infections at 3 days postinoculation (DPI).

TABLE 1 Properties of isogenic influenza viruses with different LPAI viral HA subtypes

Virus[a]	Subtype	Peak MDCK titer[b]	MLD_{50}[b]	Titer in lung[b]		SP-D binding HAI (μg)	Pathology score and rating[c]
				3 days p.i.	5 days p.i.		
H1[PB2-627E]	H1N1	7.4	>4	4.5 ± 0.7	5.3 + 0.3	ND[d]	0 (WNL)
H1	H1N1	7.3	1.8	6.8 ± 0.2	6.3 ± 0.3	>8	3 (Sev)
H1b	H1N1	6.7	2.5	ND	ND	ND	3 (Sev)
H2	H2N1	6.5	>4	3.4 ± 0.2	3.0 ± 0.0	ND	1.5 (Mod)
H3	H3N1	5.8	>4	6.0 ± 0.3	4.6 ± 0.2	4	2 (Mod)
H4	H4N1	NR[d]					
H5	H5N1	7.5	>4	6.1 ± 0.8	5.6 ± 0.3	>8	2 (Mod)
H6	H6N1	7.9	2.5	7.0 ± 0.2	6.7 ± 0.0	>8	3 (Sev)
H7	H7N1	7.7	2.5	6.7 ± 0.1	6.4 ± 0.6	>8	3 (Sev)
H7-Anhui	H7N1	6.9	2.3	6.9 ± 0.2	7.0 ± 0.2	ND	3 (Sev)
H7-Shanghai	H7N1	6.6	1.5	6.4 ± 0.4	7.5 ± 0.1	>8	2.5 (Sev)
H8	H8N1	NR					
H9	H9N1	6.75	>4	4.8 ± 0.5	3.1 ± 0.1	ND	1.75 (Mod)
H10	H10N1	7.25	1.6	7.3 ± 0.15	6.2 ± 0.3	>8	2.5 (Sev)
H11	H11N1	7.3	>4	4.5 ± 0.5	3.1 ± 0.1	ND	1 (Mild)
H12	H12N1	NR					
H13	H13N1	5.9	>4	4.3 ± 0.3	5.1 ± 0.5	ND	2 (Mild)
H14	H14N1	7.7	>4	5.1 ± 0.2	4.0 ± 0.1	ND	1 (Mild)
H15	H15N1	7.2	3.6	5.1 ± 0.2	4.2 ± 0.3	>8	2.5 (Sev)
H16	H16N1	7.4	>4	5.3 ± 0.2	4.4 ± 0.1	ND	0.5 (Mild)

[a] Influenza A viruses were constructed using the 7 gene segments of the LPAI virus H1N1 parental virus with the PB2 E627K mutation (except where noted) but expressing the HA genes of LPAI viruses of different subtypes, as indicated; see Table S1 in the supplemental material.

[b] Data are presented as $\log_{10}$ PFU.

[c] See Materials and Methods for description of pathology score (range, 0 to 3). Sev, severe influenza pneumonia; Mod, moderate influenza pneumonia; Mild, mild influenza pneumonia; WNL, within normal limits (no pathological changes).

[d] ND, not determined; NR, not rescued. AI[PB2-627K] viruses bearing H4, H8, and H12 subtype HAs could not be recovered by reverse genetics in this study.

infections: both of the H1 viruses (H1 and H1b), along with the H6, H7, and H10 viruses (Fig. 1C). Viruses expressing the other HA subtypes (H2, H3, H5, H9, H11, H13, H14, H15, and H16) caused mild weight loss (<10% maximum weight loss) and no fatalities at a dose of 10^3 PFU. A comparative MLD_{50} study was next performed, which showed that the H6, H7, and H10 viruses had MLD_{50} of 2.5, 2.5, and 1.6 $\log_{10}$ PFU, respectively (Table 1) ($n = 5$ per dose for each virus). Infection with the H15 virus also led to fatal infections (MLD_{50} of 3.6 $\log_{10}$ PFU). The remaining viruses (H2, H3, H5, H9, H11, H13, H14, and H16) had an undetermined MLD_{50} (>4 $\log_{10}$ PFU, the highest dose tested).

Because the H7 virus (expressing a North American H7 LPAI viral HA) was pathogenic in mice, we evaluated two additional isogenic chimeric viruses expressing H7 genes derived from two 2013 Chinese H7N9 human isolates, A/Anhui/1/2013 (H7N9) and A/Shanghai/1/2013 (H7N9), on the same genetic background as the other viruses (Fig. 1D; see also Table S1 in the supplemental material). Both of these chimeric H7 viruses were pathogenic in mice (MLD_{50} of 2.3 and 1.5 $\log_{10}$ PFU, respectively) (Table 1) ($n = 5$ per group).

Titers of virus in lung were determined at 3 and 5 days postinfection (p.i.) (Table 1) ($n = 3$ for each time point in each group). All the viruses replicated in mouse lung, with titers ranging from 3.0 to 7.5 $\log_{10}$ PFU/g lung tissue. Chimeric viruses expressing the HA subtypes (H1, H6, H7, H10, and H15) resulting in pathogenic infections generally replicated to higher titers in lung than the viruses expressing the remaining HA subtypes (Fig. 1E), but there was no clear relationship between lung titers at 3 and 5 days p.i. and disease severity. For example, at 3 days p.i., the H3 and H5 viruses replicated to titers very similar to those for the pathogenic H1, H6, H7, and H10 viruses, while viral titers for the pathogenic H15 virus were approximately 2 $\log_{10}$ PFU/g lower, comparable to titers observed with the nonpathogenic H11, H13, and H16 viruses (Table 1; Fig. 1E).

Comparison of viruses with glutamic acid at PB2 amino acid 627 in mice. The PB2 E627K mutation has long been associated with mammalian adaptation (28) and pathogenicity of some highly pathogenic H5N1 viruses (34) and the reconstructed 1918 pandemic virus in mice (15). As shown, the H1[PB2-E627] avian consensus virus was apathogenic in mice, while the isogenic virus containing PB2 K627 was quite pathogenic and replicated to titers 1 to 2 $\log_{10}$ PFU/g higher (Fig. 1B and Table 1). To test whether the HA-associated pathogenicity observed with viruses expressing not only H1 but also H6, H7, H7-Shanghai, H7-Anhui, H10, and H15 HAs would also be seen with a set of isogenic viruses encoding PB2 E627, viruses were constructed, and mice were inoculated with 10^3 PFU intranasally, 5 per group. In all cases, mice lost ≤10% of initial body weight and no lethal infections were observed (see Fig. S2A in the supplemental material). Similarly, the parental wild-type LPAI H1N9, H5N1, H6N1, H7N3, and H10N8 viruses (see Table S1) were not pathogenic in mice. Mice lost ≤8% of initial body weight, and no lethal infections were observed (see Fig. S2B).

SP-D hemagglutination inhibition *in vitro*. The mannose-containing influenza A virus surface glycoproteins HA and NA can be recognized by components of innate immunity in the respiratory system, including collectin family lectins like surfactant protein D (SP-D), expressed by alveolar type II epithelial cells and Clara cells. SP-D was previously shown to bind carbohydrate residues on some influenza A viruses, likely leading to aggregation and clearance (35). In a previous study, we demonstrated that isogenic influenza viruses expressing the HAs of the 1918, 1957,

1968, and 2009 pandemics showed low binding activity for SP-D and this was correlated with viral replication in alveolar epithelial cells (22). Since viral replication in the lower respiratory tract was correlated with enhanced pathogenicity in that study, we sought to determine if SP-D inhibition could be correlated with the pathogenicity of the isogenic avian HA-expressing chimeric viruses evaluated here. SP-D hemagglutination inhibition assays were performed with the pathogenic H1, H6, H7, H7-Shanghai, H10, and H15 viruses along with the less pathogenic H3 and H5 viruses. For the avian viruses evaluated (Table 1), SP-D could not inhibit hemagglutination at the highest SP-D concentrations tested (4 to 8 μg), in marked contrast to a control seasonal H1N1 virus, which was inhibited with 0.0625 μg (22).

Lung histopathology. Histopathologic changes to the respiratory system induced following mouse infection with the isogenic H1 to H16 viruses were evaluated using a lung pathology scoring system of 0 to 3 (where 0 represented no pathology, and 3 represented severe pathology and the greatest degree of tissue involvement; the average score was derived from two replicate mice per group evaluated independently by two pathologists), 2 per time point for each virus. A score of <1.5 reflected mild influenza pneumonia, a pathology score of 1.5 to 2.25 reflected moderate influenza pneumonia, and pathology scores of >2.25 reflected severe influenza pneumonia. The parental LPAI virus H1N1 virus (H1$^{PB2-627E}$) induced no pathological changes (pathology score of 0). In contrast to the case with titers in lung, there was a good correlation of high pathology score and low MLD$_{50}$ with the pathogenic viruses, since infections with the H1, H6, H7, H10, and H15 viruses each resulted in severe pneumonias (pathology scores of 2.5 to 3). The remaining viruses had pathology scores ranging from 0.5 to 2, reflecting mild influenza pneumonia (H11, H14, and H16) or moderate influenza pneumonia (H2, H3, H5, H9, and H13) (Table 1). Examples of avian viruses that induced severe influenza pneumonia in mice are shown in Fig. 2: H1, H7, H7-Anhui, H7-Shanghai, H6, and H10 (Fig. 2A to F, respectively). In these animals, pathological changes involved up to 50% of the lung parenchyma with multifocal, moderate to severe, necrotizing bronchitis and bronchiolitis along with moderate to severe alveolitis with multifocal pulmonary edema and fibrinous exudates. The alveolar inflammatory infiltrates were of mixed cellularity, and airspace neutrophils and macrophages were commonly observed (Fig. 2A, inset). The H5 virus was representative of those viruses that induced a moderate influenza pneumonia pattern (Fig. 2G). Pathological changes in these animals involved <25% of the lung parenchyma and demonstrated multifocal, predominantly lymphohistiocytic, mild to moderate alveolitis and bronchiolitis and bronchitis. The parental H1N1 LPAI virus (H1$^{PB2-E627}$) induced no pathological changes (Fig. 2H).
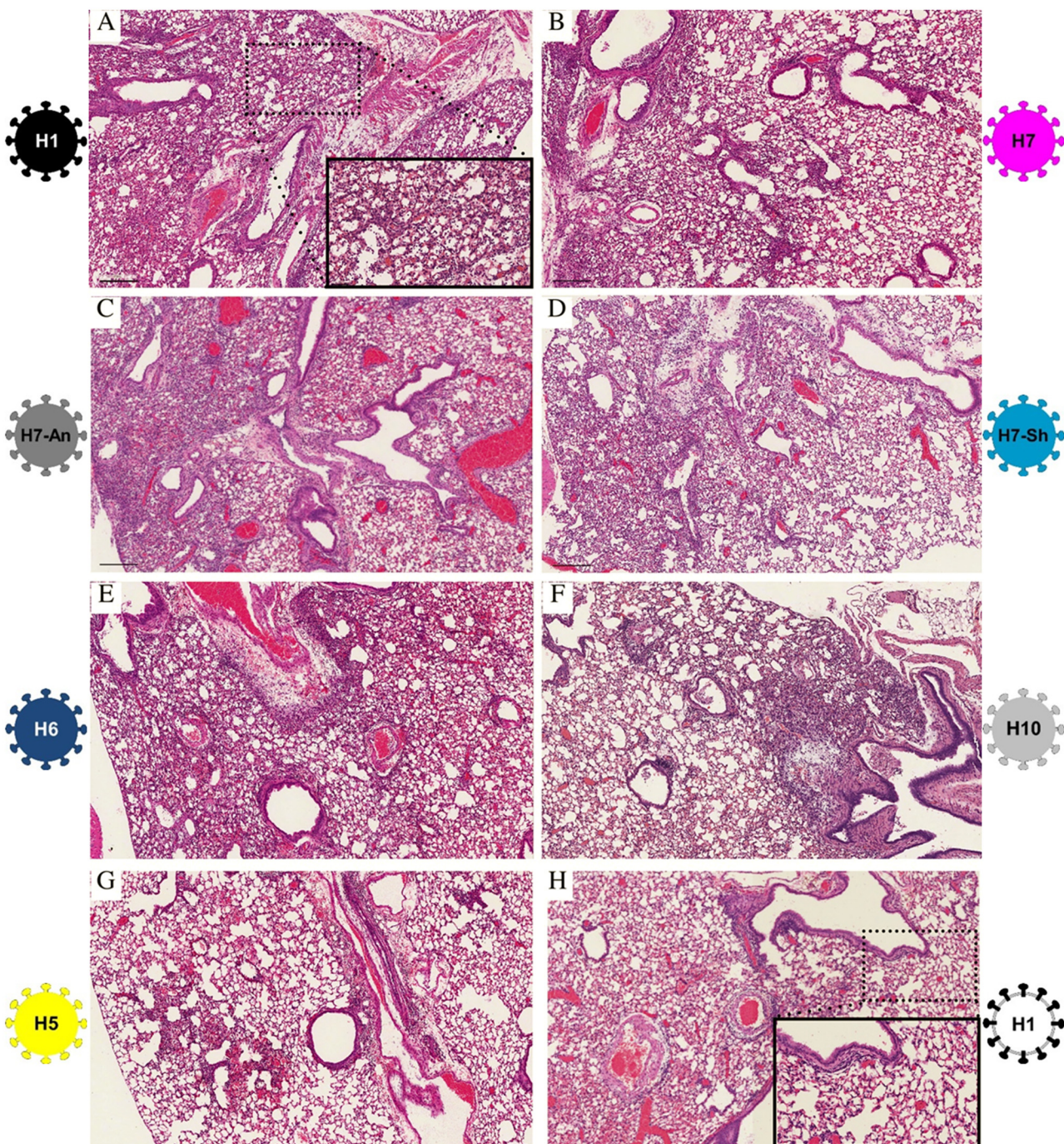
Immunophenotypic analyses of lung inflammatory cells in infected mice. Because the isogenic viruses expressing the H1, H6, H7, H10, and H15 subtypes induced severe influenza pneumonias with prominent inflammatory infiltrates, while the isogenic viruses expressing the other HA subtypes did not, mice infected by representative pathogenic viruses (H1 and H7) and less pathogenic viruses (H3 and H5) were characterized by flow cytometry to determine the distribution of immune cells present in the lung. Mice were infected with 10^3 PFU of these representative viruses or 50 μl of Dulbecco's modified Eagle's medium (DMEM) as a mock control. At 6 days p.i., mice were euthanized and peripheral blood was flushed from the lungs ($n = 5$ per group). Single-cell lung suspensions were analyzed by flow cytometry. As shown, lung immune cells (CD45$^+$) increased following infection compared to homeostatic levels seen in mock-infected lungs (Fig. 3A). All of the viral infections evaluated resulted in an increase in CD45$^+$ cells at 6 days p.i. compared to results for mock-infected animals, although the H5 virus did not reach significance compared to mock infection, as determined by Tukey's multiple comparisons. Moreover, the number of CD45$^+$ cells in H1-infected mice was significantly higher than those in H3- and H5-infected mice ($P = 0.0005$ and $P = 0.0025$, respectively). H7-infected mice also exhibited a higher level of CD45$^+$ lung cells than H5-infected mice ($P = 0.0007$). These results showed that the more pathogenic H1 and H7 viruses led to increased immune cell recruitment and/or proliferation than the less pathogenic H3 or H5 viruses despite similar titers of virus in lung (Fig. 1D).

The total population of CD45$^+$ cells was then further phenotyped to assess the distribution of different immune cells present in the lungs at 6 days p.i. Overall, the mock-infected mice had higher proportions of resident macrophages (CD11c$^+$ SiglecF$^+$) and B cells (CD11c$^-$ CD3$^-$ CD19$^+$) than the four groups of infected mice (Fig. 3B, first row). Remarkably, the H3 and H5 infections did not appear to drastically alter the proportions of immune cells seen during homeostasis, since CD4 T cells (CD11c$^-$ NKp46$^-$ CD3$^+$ CD8$^-$ CD4$^+$) and CD8 T cells (CD11c$^-$ NKp46$^-$ CD3$^+$ CD4$^-$ CD8$^+$) were present in H3- and H5-infected mice in the same proportion as in mock-infected mice; NK cells (CD11c$^-$ CD3$^-$ NKp46$^+$) were more abundant than the other groups (Fig. 3B, second and third rows). Mature dendritic cells (DCs) (CD11c$^+$ SiglecF$^-$ I-A^{d+}) were more abundant following infection with all four viruses; however, DCs were present in significantly higher proportions following H1 and H7 infection than following infection with H3 or H5 (Fig. 3B, third row). Infection with the more pathogenic H1 and H7 viruses resulted in a large proportion of neutrophils (CD11c$^-$ SiglecF$^-$ CD11b$^+$ Ly6G/C^{hi}) and inflammatory macrophages (CD11c$^-$ SiglecF$^-$ CD11b$^+$ Ly6G/C^{mid}) (Fig. 3B, fourth row).

In addition to analyzing proportions of CD45$^+$ cell populations, the total number of neutrophils and inflammatory macrophages present were analyzed. H1- and H7-infected mice had significantly more inflammatory macrophages than mock-, H3-, and H5-infected animals, and H1-infected animals had significantly more neutrophils than mock-, H3- and H5-infected animals (Fig. 3C). H7-infected mice had significantly more neutrophils than mock- and H5-infected animals, with a trend of more neutrophils as compared to that for H3-infected mice.
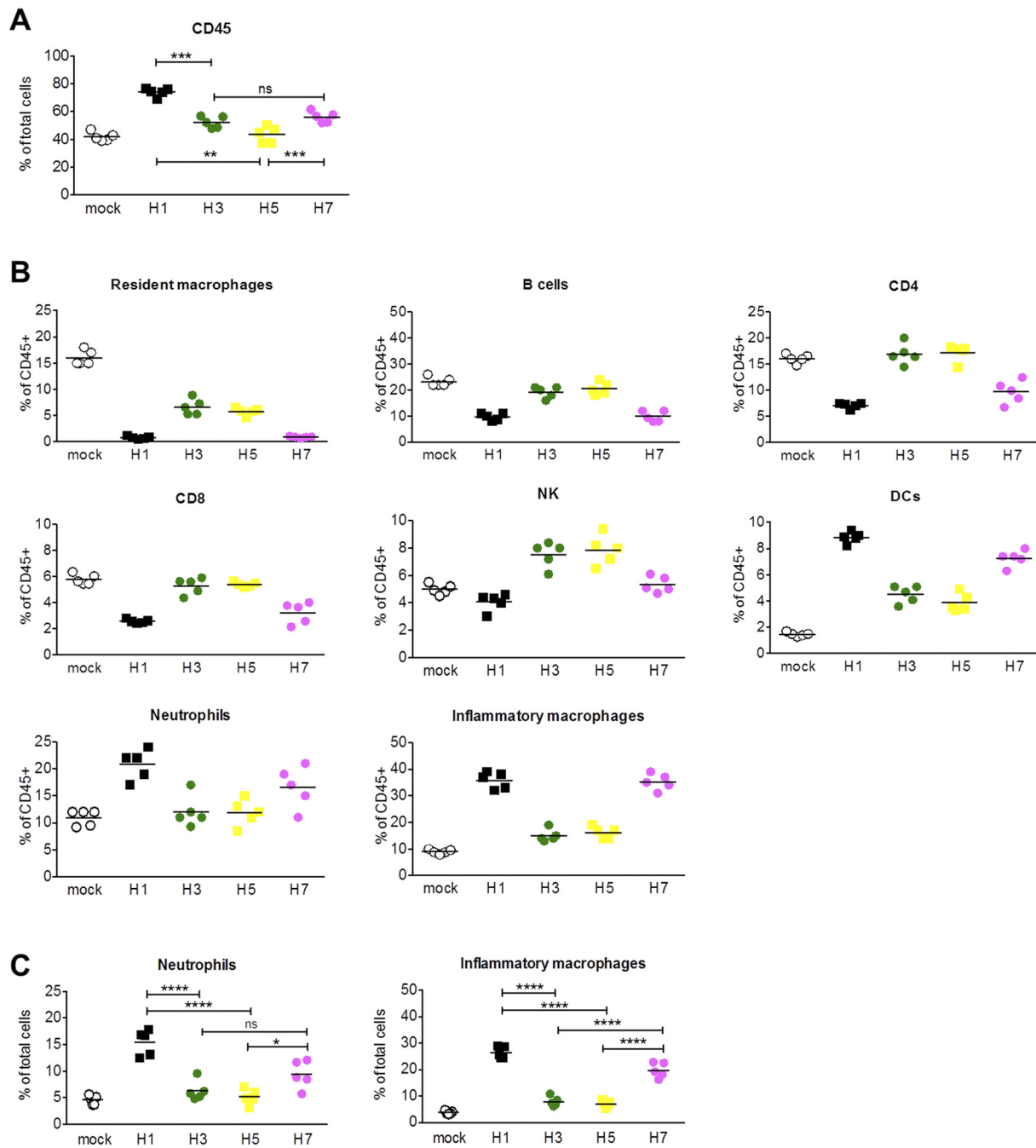
Global gene expression analysis of lung RNA. To characterize the host response to infection, we performed expression microarray analyses with a subset of viruses, including the parental LPAI virus H1$^{PB2-627E}$, the pathogenic viruses H1, H6, H7, and H10, and the mildly pathogenic H3 and H5 viruses. Groups of mice, 5 at each time point, were infected with 10^3 PFU of each virus, and lungs were collected at 1, 3, and 6 days p.i. Total RNA was isolated from 3 mice per group, and mRNA expression microarray analysis was performed. All viral infections resulted in activation of type I interferon (IFN) responses (Fig. 4A) with similar expression levels of many type I IFN-related genes, such as those encoding the type I IFN receptor (*Ifnar1* and *Ifnar2*), the associated kinase Jak1, and the transcription factor Irf3 and several interferon-induced genes (ISGs), including *Ifi30*, *Ifitm2*, and *Ifitm3* (see Fig. S3 in the supplemental material). The pathogenic H1, H6, H7, and H10 viral

FIG 2 Representative histopathologic changes observed in mouse lung following infection with representative chimeric avian influenza A viruses investigated in this study. Photomicrographs of hematoxylin-and-eosin-stained sections of mouse lung at 5 days p.i. following intranasal inoculation with 10^3 PFU of chimeric viruses; bars = 200 μm. (A) Marked influenza virus pneumonia following infection with the H1 virus, showing alveolitis with prominent airspace neutrophils and macrophages (inset). (B to F) Histopathologic changes similar to those seen following H1 infection with H7, H7-Shanghai, H7-Anhui, H6, and H10 viruses, respectively. (G) Moderate influenza virus pneumonia pattern following infection with the H5 virus. (H) Lung section showing no pathological changes following infection with the H1$^{PB2-E627}$ virus; inset shows normal alveoli without inflammatory infiltrates.

infections resulted in higher expression levels for many other double-stranded RNA (dsRNA) and type I IFN response genes, such as *Ifih1*, *Ddx58*, *Irf7*, and *Mx1* (see Fig. S3). All viral infections resulted in the increased expression of cytokine and chemokine genes compared to results with lungs of mock-infected animals.

The H1, H6, H7, and H10 viral infections were also associated with significantly more robust induction of genes related to reactive oxygen species (ROS) and nitric oxide (NO) responses (Fig. 4A). Examination of genes associated with activation of specific immune cells showed that infection with H1, H6, H7 or H10
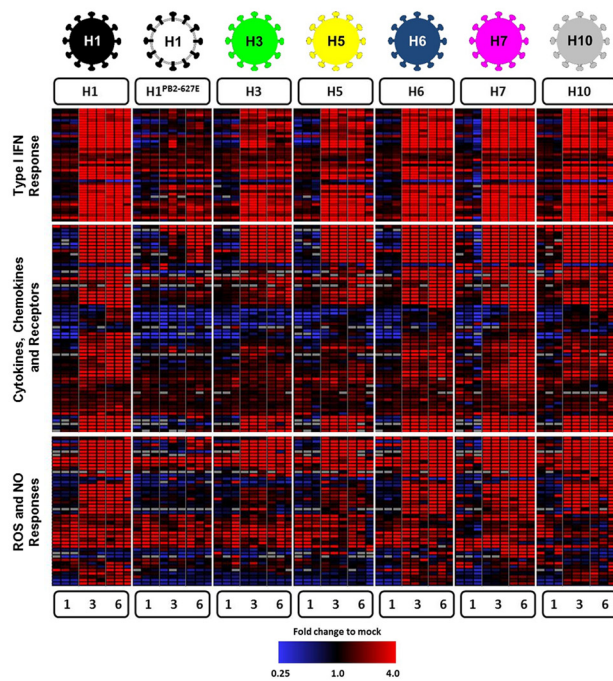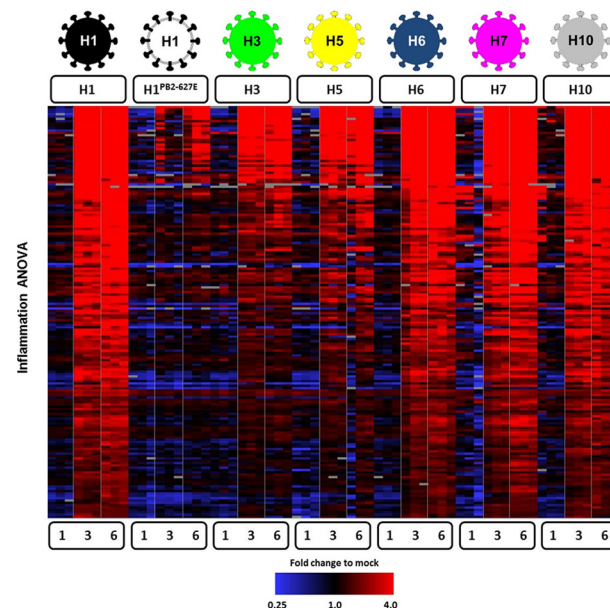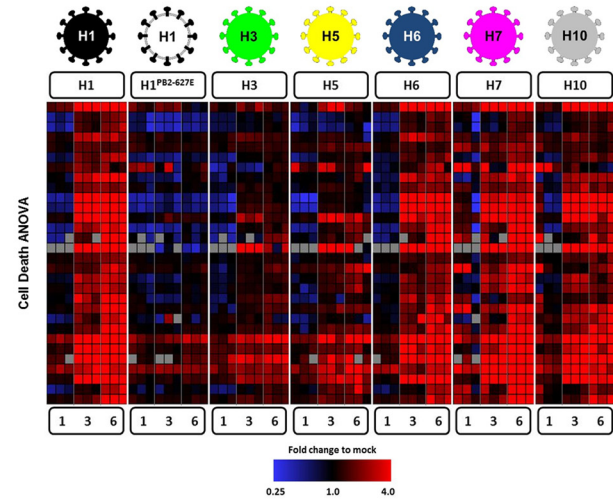
FIG 3 Immunophenotypic analysis of lung CD45$^+$ cells following infection with chimeric avian influenza viruses, at 6 days p.i. (A) Percentage of lung cells that were CD45$^+$ at 6 days p.i. following infection with the H1, H3, H5, and H7 viruses, compared to those for mock-infected animals. H1, H3, and H7 infections resulted in a statistically significant increase in CD45$^+$ cells compared to mock infection. (B) Percentage of lung CD45$^+$ cells by immune cell phenotype. Mature DCs H1 versus H3, $P = 0.0005$; H1 versus H5, $P = 0.0002$; H7 versus H3, $P = 0.0109$; H7 versus H5, $P = 0.0042$. (C) Total percentage of neutrophils and activated macrophages. Both neutrophils and inflammatory macrophages were present in significantly higher percentages in the lungs from the pathogenic H1 and H7 infections than in those from the less pathogenic H3 and H5 infections. For neutrophils: H1 versus H3, $P < 0.0001$; H1 versus H5, $P < 0.0001$; H7 versus H3, $P = 0.1415$; H7 versus H5, $P = 0.0226$. For inflammatory macrophages: H1 versus H3, $P < 0.0001$; H1 versus H5, $P < 0.0001$; H7 versus H3, $P < 0.0001$; H7 versus H5, $P < 0.0001$.

viruses resulted in a more potent activation of macrophages and neutrophils compared to that in H1$^{PB2-627E}$, H3, or H5 viral infections (see Fig. S4), consistent with flow cytometric analyses.

While infection with all viruses tested resulted in the activation

of antiviral and immune responses, the H1, H6, H7, and H10 viral infections also all caused higher expression of many host response genes. To identify the population of genes that showed significantly higher expression in these more virulent infections, analysis
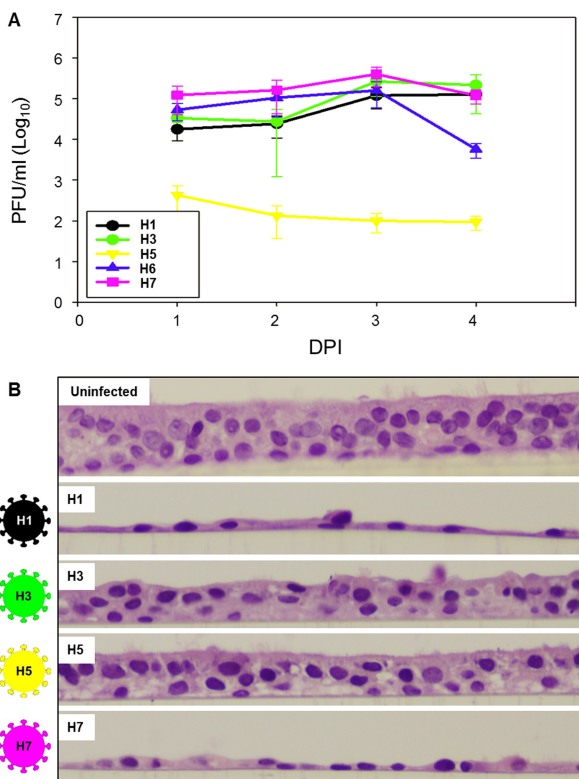
FIG 4 Analysis of gene expression responses in mouse lung tissue. Expression microarray analysis was performed with total RNA isolated from lungs of three mice per group collected at days 1, 3, and 6 postinfection with H1, H1^PB2-627E, H3, H5, H6, H7, and H10 viruses compared to a pool of RNA isolated from uninfected mouse lung tissue. (A) Immune response genes, including type I IFN, cytokines, chemokines, and cognate receptors, and ROS and NO responses. (B) Inflammatory response-related genes identified by ANOVA (using adjusted Bonferroni error correction with $P = 0.01$) as having statistically significant differential expression in the H1, H6, H7, and H10 compared to H3 and H5 viral infections at days 3 and 6 postinfection. (C) Cell death response-related genes identified by ANOVA (using adjusted Bonferroni error correction with $P = 0.01$) as having statistically significant differential expression in the H1, H6, H7, and H10 compared to H3 and H5 viral infections at day 6 postinfection. Genes shown in red were upregulated, genes shown in blue downregulated, and genes in black indicate no change in expression in infected relative to uninfected animals.

of normal variance (ANOVA) was performed. As shown in Fig. 4B, the H1, H6, H7, and H10 viruses resulted in significantly higher expression of many inflammatory response genes, including *Il1b* and *Il12b*, than the H1^PB2-627E, H3, and H5 viruses. Moreover, many of the most highly expressed genes in the H1, H6, H7, and H10 viral infections were associated with activation of monocytes and neutrophils, such as *Cxcl9*, *Cxcl10*, *Cxcl11*, *Ccl2*, *Ccl3*, *Ccl4*, and *Ccl7* (see Fig. S4 in the supplemental material), again

consistent with the flow cytometric analysis showing increased levels of these activated immune cells associated with the pathogenic viruses. ANOVA also revealed that the H1, H6, H7, and H10 viral infections induced more significant cell death-related gene expression responses, including *Casp1*, *Daxx*, *Ripk3*, and *Tnf*, than the H1^PB2-627E, H3, and H5 infections (Fig. 4C).

Kinetics and cytopathicity of chimeric avian influenza virus-infected NHBE cell culture. To evaluate whether the observed

FIG 5 Infection of differentiated normal human bronchial epithelial (NHBE) primary cell cultures. (A) Replication kinetics of chimeric avian influenza H1, H3, H5, H6, and H7 viruses in NHBE cell culture. Lung titers (PFU/ml) determined on days 1 to 4 postinfection (DPI), following infection with an MOI of 1 at time zero. (B) Histopathology of NHBE cell cultures at 72 h after infection with H1, H3, H5, or H7 viruses at an MOI of 1; original magnification, ×400. The cultures infected with the H1 and H7 viruses show only remnant basal cells, while the H3 and H5 infections show maintenance of a pseudostratified epithelium but with fewer ciliated cells, pyknotic nuclei, increased cytoplasmic vacuolization, and apparent separation of overlying cells from the basal cell layer.

pathogenicity of avian HA-expressing influenza viruses was restricted to mice, *in vitro* infections of representative pathogenic and less pathogenic viruses were performed in differentiated normal human bronchial epithelial (NHBE) cell cultures, in triplicate. Differentiated NHBE cells grown at the air-fluid interface *in vitro* demonstrated a pseudostratified epithelium with visible ciliated cells, goblet cells, and basal cells. NHBE cultures were infected with H1, H3, H5, and H7 viruses at a multiplicity of infection (MOI) of 1. The H1, H3, and H7 viruses replicated to 5-6 $\log_{10}$ PFU/ml (Fig. 5A), while the H5 virus replicated to lower titers. In contrast, viral infection induces cytopathic changes to the NHBE cells. Interestingly, the H1 and H7 viruses induced markedly more cytopathicity in the NHBE cultures than the H3 and H5 viruses (Fig. 5B), with the pseudostratified epithelial cell layer reduced to only basal cells by 72 h after infection, correlating well with the observed mouse pathogenicity.

DISCUSSION

Influenza pandemics have emerged at least 15 times in the last 500 years (36), and increasing surveillance in recent years has facilitated identification of a number of influenza A virus zoonotic

outbreaks of avian origin (7, 8) or swine origin (37). The mechanisms of influenza A virus stable host switch are not well elucidated (6), but for a sustained outbreak to occur, zoonotically derived viruses must be able to infect host cells in the new species, replicate, and be transmitted between humans (5). It is likely that viral properties including replication, pathogenicity, and transmissibility are polygenic traits driven by mutational pressures that are independent and possibly competing (5). These factors may have contributed to the variable morbidity and mortality impact of past influenza pandemics and current zoonoses. Understanding the molecular basis of host switch events is an important public health goal to prevent or mitigate an outbreak prior to the emergence of a full-blown pandemic. However, the basis for variable pathogenicity of pandemic and zoonotically derived influenza A virus strains is not well understood.
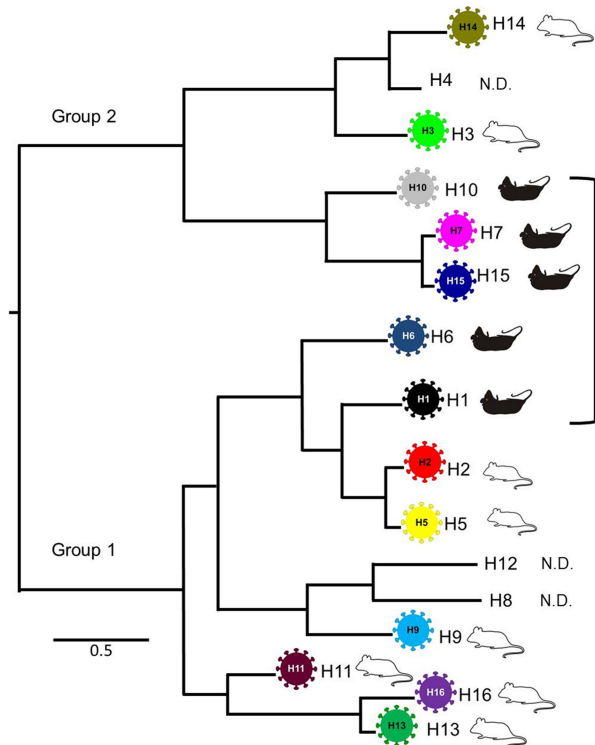
The 1918 "Spanish" H1N1 influenza pandemic was the worst pandemic in recorded history, with a global mortality of approximately 50 million people (13) associated with unusual case fatality in young adults (38). The fully reconstructed 1918 pandemic virus is pathogenic without adaptation in mice, ferrets, and macaques and is associated with markedly increased proinflammatory, cell death, and ROS responses in the lungs of these experimental animals and suppression of type I IFN responses in bronchial epithelial cells (23, 26, 39, 40). While the 1918 HA has been identified as a key virulence factor in mammalian models (15, 20–23), an H1 subtype HA from an LPAI virus did not attenuate a 7:1 1918 chimeric virus (15). In the current study, an LPAI H1N1 virus with a single coding change in the polymerase PB2 (E627K) to facilitate viral replication in mouse lung was shown to be equally as pathogenic as the fully reconstructed 1918 virus in mice. Further, inherent mammalian virulence associated with the avian influenza virus H1 was also observed in isogenic chimeric viruses expressing H6, H7, H10, and H15 HAs. These data support the hypothesis that a key virulence feature of the 1918 virus is not unique to the HA in the pandemic virus but is shared with circulating LPAI virus H1 HAs and LPAI virus HAs of H6, H7, H10, and H15 subtypes as well. The variable pathogenicity observed with these chimeric avian viruses did not correlate with SP-D hemagglutination inhibition, suggesting other mechanisms for the observed pathogenicity. The chimeric viruses evaluated in this study would be unlikely to infect wild mice, since they express Mx1 (41).

The otherwise isogenic LPAI virus chimeras expressing the H1, H6, H7, H10, and H15 HA subtypes share common pathogenic properties with the reconstructed 1918 human pandemic influenza virus in mice. In addition to low MLD_{50} values ($<10^3$ PFU), they induced severe viral pneumonia with a marked inflammatory infiltrate, including increased numbers of macrophages and neutrophils, as seen previously with 1918 influenza virus infections (15, 40), and confirmed in this study by flow cytometric analysis, and changes in whole lung gene expression patterns associated with enhanced inflammatory, ROS, and cell death responses. The analysis of the host gene expression response to infection showed several key features associated with the more pathogenic H1, H6, H7, and H10 infections. In general, gene expression responses to all viruses evaluated showed activation of dsRNA and type I IFN and immune responses; however, these antiviral responses had little impact on reducing viral replication. Previous studies have shown that the 1918 influenza virus, which expresses an NS1 protein very close to the avian influenza virus consensus sequence

(15), is a potent inhibitor of dsRNA and type I IFN responses in infected human cells or nonhuman primates (26, 42). Similar to findings in studies with the 1918 virus, the more pathogenic H1, H6, H7, and H10 viral infections were associated with significantly higher expression of proinflammatory cytokines and chemokine mRNAs (see Fig. S3 and S4 in the supplemental material). Also consistent with the inflammatory response to the 1918 virus, higher gene expression associated with recruitment and activation of macrophages and neutrophils was also observed with the avian H1, H6, H7, and H10 viruses. Neutrophils and macrophages were also demonstrated to be present at statistically higher levels in these infections by flow cytometry and corroborated by histopathology. Previous studies have shown that activation of these immune cell types, particularly neutrophils, is an important feature of 1918 influenza viral infections in animal models (25, 27, 40). Similarly, neutrophilic alveolitis was also commonly observed in 1918 human autopsy samples (43, 44). Thus, a key driving force of primary severe lung pathology resulting from certain influenza virus infections, such as infection with the 1918 virus, are likely related to activation of macrophages and neutrophils with concomitant activation of ROS and cell death responses. Supportive of this view, we reported that mice infected with a lethal dose of the 1918 influenza virus and treated with the catalytic catalase/superoxide dismutase mimetic organometallic drug EUK-207 had greatly increased survival and reduced severity of lung pathology, particularly ROS damage of alveolar epithelial cells (39). In future work, it would be interesting to evaluate these isogenic viruses for differential replication and alterations in host gene expression in macrophages *in vitro*.

Intriguingly, we also observed marked differences in the cytopathicity of these chimeric avian viruses in differentiated primary NHBE cells, demonstrating that expression of different HAs can directly affect cell death and/or autophagy responses in primary human lung epithelial cells. This suggests that increased activation of cell death gene expression responses observed in H1-, H6-, H7-, and H10-infected mouse lungs likely results from both directly cytopathic viral infection and immune cell killing via macrophages and neutrophils. Additional studies are under way to determine the mechanisms underlying these observations. The HA subtypes associated with enhanced pathogenicity are genetically divergent and include both group 1 and group 2 subtypes, but it is possible that there are shared structural or physiological features that might underlie the enhanced pathogenesis observed. Some possibilities include differential glycosylation patterns, differences in pH optima of fusion, or differential cell entry. Moreover, the *in vitro* results indicate that the enhanced pathogenicity of H1, H6, H7, and H10 viruses is not limited to experimental mouse infections, and these HA subtypes could contribute to enhanced pathogenicity observed in humans in some avian influenza virus zoonotic infections. Taken together, these findings suggest that several independent factors are critical for development of a pathogenic phenotype when an LPAI virus adapts to a mammalian host—polymerase adaptations, inhibition of antiviral responses to enhance viral replication, and an HA from one of the above subtypes to exert an independent virulence property that triggers cell death and robust inflammatory responses.

Influenza A virus HA subtypes did not evolve from a common ancestor in a single radiation and also demonstrate higher-order clustering into two larger, deeply divergent clades (4). Interestingly, the avian HA subtypes associated with increased pathoge-


FIG 6 Representative avian influenza A virus hemagglutinin phylogenetic tree. Tree topology is based on the work of Dugan et al. (4). Chimeric avian influenza viruses with HA subtypes associated with mouse pathogenicity are indicated by black mice and enclosed with the bracket; viruses associated with less pathogenicity are indicated by white mice. N.D., not determined.

nicity are found in both higher-order clades 1 and 2 but are clustered in two smaller subclades, a clade 1 subclade containing H1 and H6 and a clade 2 subclade containing the H7, H10, and H15 HAs (Fig. 6). The observed clustering of these HA subtypes suggests the possibility that these five HA subtypes might share some sequence and/or structural feature(s) contributing to the observed mammalian virulence. In the future, it would be interesting to examine the role of HA/NA interactions in the context of pathogenicity with other avian influenza NA subtypes, since all the chimeric viruses evaluated here expressed the identical N1 subtype NA.

Recent zoonotic outbreaks associated with LPAI viral infections of H7N9, H10N8, and H6N1 have been associated in many cases with substantial morbidity and mortality. In the last year, 2013-2014, H7N9 infections have been documented in 375 people as of 8 April 2014 (45), with 115 deaths (30.6% case fatality rate). The H7N9 viruses are LPAI viruses without an HA polybasic cleavage site, but significantly, the majority of human isolates have contained the PB2 E627K mutation (46) (35/48; 73% of sequences in GenBank), and several cases without E627K have the mammal-associated PB2 mutation D701N (47, 48). During the 2003 H7N7 outbreak in the Netherlands, sequence analysis of the virus isolated from the single human fatality also contained a PB2 E627K mutation (49). A fatal infection with an H10N8 LPAI virus was also recently reported (50), and the isolate was also shown to encode a PB2 E627K mutation (12). Prior human or mammalian infections with H10 LPAI viruses have been rare, but a large and

highly fatal H10N4 outbreak occurred in mink farms in Sweden in 1984 (51). Recently, viral sequences from that outbreak were shown to contain a PB2 D701N mutation (52). A documented H6N1 human infection was also recently reported (10), raising concern about zoonotic potential of H6 LPAI viruses (53). Interestingly, LPAI H6 strains have been associated with mouse and ferret pathogenicity (53–55), as have LPAI H1N1 strains (56). Given the rapid accumulation of the PB2 E627K mutation during mouse infections with the $1918^{\text{AI-PB2}}$ virus (15) or H5N1 viruses (57), it would be of interest to examine sequences of the viral polymerase genes during the course of infection from lung-derived isolates in the above mouse LPAI H1 and H6 studies.

The 16 HA subtypes found in wild aquatic birds are not uniformly distributed. HA subtypes H1, H6, H7, H10, and H15 collectively account for ~40% of LPAI viruses in large ecological surveys (3, 58), with H6 being most commonly observed, H1, H7, and H10 subtypes being less common, and H15 being rare. It is therefore likely that a sizeable fraction of human exposure to LPAI viruses involves strains expressing one of these five HA subtypes. In the murine infections evaluated here, the isogenic chimeric LPAI viruses (with the single PB2 E627K mutation to facilitate replication) that expressed one of these five HA subtypes resulted in a pathological phenotype very similar to or indistinguishable from that of the 1918 pandemic virus, supporting and expanding the hypothesis that 1918-like LPAI viruses circulate in wild birds (15, 59). However, despite countless exposures at the human-animal interface, pandemic influenza viruses emerge very infrequently.

This suggests that the pathway for an avian influenza A virus to become a pandemic strain is an extremely complex, multifactorial process not easily achieved. Ecological and biological constraints still poorly understood likely limit emergence of pandemic influenza viruses, including adaptations to intermediate hosts as well as the acquisition of human adaptations that facilitate replication and ultimately transmissibility. Despite this complexity, severe influenza pandemics like that of 1918 have occurred in the past and consequently may occur in the future. The data presented here support the hypothesis that zoonotic AI virus infections caused by AI viruses expressing the H1, H6, H7, H10, or H15 subtype might be associated with enhanced morbidity in humans. Enhanced surveillance is important to characterize novel viruses at the animal-human interface, but ultimately, a broadly reactive "universal" influenza vaccine may offer the best protection against future pandemics (60).

MATERIALS AND METHODS

Virus preparation. A set of isogenic chimeric rescued "7:1" viruses was prepared using standard reverse genetics as previously described (15). All rescued viruses constructed for this study contained the same seven gene segments (PB1, PB2, PA, NP, NA, M and NS) from an LPAI virus (influenza A/Green Wing Teal/Ohio/175/1986 [H2N1]) (15). This parental AI virus was chosen because the "internal" genes of this virus were each very similar to AI virus consensus sequences (15). In each case (except where indicated), the PB2 gene contained the E627K mutation to facilitate replication in mouse lungs (15). The isogenic viruses expressing H1 to H3, H5 to H7, H9 to H11, and H13 to H16 HA subtype genes were successfully rescued. Chimeric viruses possessing H4, H8, and H12 were not able to be rescued. A summary of the HA donor strains is shown in Table S1 in the supplemental material. Full-length HA gene segments (except for H14 and H15) from the LPAI viruses were produced by reverse transcription PCR (RT-PCR) and cloned into pHH21 vectors as described elsewhere

(15). HA genes of the H14 and H15 subtypes were synthesized (GenScript, Piscataway, NJ) prior to cloning into pHH21 vectors. The HA genes from two recent human H7N9 isolates were also produced by RT-PCR from the A/Anhui/1/2013 (H7N9) strain, and this clone was subsequently mutagenized to match the A/Shanghai/1/2013 (H7N9) HA sequence (nine coding changes). The chimeric viruses were grown in Madin-Darby canine kidney (MDCK) cells for 1 to 2 passages. The genomic sequence of each rescued virus was then confirmed by sequence analysis of the inoculum. All viruses and infectious samples were handled under enhanced biosafety level 3 (BSL-3) laboratory conditions, in accordance with the biosafety guidelines of the NIH Division of Health and Safety following approvals by the NIH Institutional Biosafety Committee. Work with these viruses was evaluated by the NIH/NIAID Division of Intramural Research and the Institutional Biosafety Committee and determined not to constitute dual-use research.

SP-D inhibition assay. Surfactant protein D (SP-D) inhibition *in vitro* was performed as previously described (22). Briefly, the minimum concentration of SP-D required to fully inhibit the hemagglutinating activity of the viral suspension was determined as previously described (22).

Mouse infection. Groups of 6- to 8-week-old female BALB/c mice (Jackson Laboratories, Bar Harbor, ME) were lightly anesthetized in a chamber with isoflurane supplemented with O_2 (1.5 liters/min) prior to intranasal (i.n.) inoculation with virus in a total volume of 50 μl. Viruses were diluted in sterile phosphate-buffered saline (PBS) or Dulbecco's modified Eagle's medium (DMEM) where appropriate. Survival and body weight were monitored for up to 14 days, and mice that lost more than 25% starting body weight met euthanasia criteria and were humanely killed. Mouse 50% lethal doses (MLD_{50}) were determined by inoculating groups of five mice with serial 10-fold dilutions of virus. MLD_{50} were calculated by the method of Reed and Muench (61) and were expressed as the log_{10} plaque-forming units (PFU) required to give 1 MLD_{50}. For the experimental animal study comparing the pathogenicity between viruses, groups of 5 mice were inoculated i.n. with 1,000 PFU of each virus. On 3 and 5 days postinoculation (p.i.), lungs from 3 animals were collected for viral titration, and on 5 days p.i., lungs from 2 additional animals were collected for pathology from each virus group. Total lung RNA was isolated from animals on 1, 3, and 6 days p.i. (see below). Viral titers in lung were determined by plaque assay in 10% (wt/vol) lung suspensions prepared by homogenization in sterile 1× L15 medium. Lungs collected for histopathology were inflated with 10% neutral buffered formalin (NBF) at the time of harvest in order to prevent atelectasis. All experimental animal work was performed in accordance with United States Public Health Service (PHS) Policy on Humane Care and Use of Laboratory Animals in an enhanced animal BSL-3 (ABSL-3) laboratory at the National Institute of Allergy and Infectious Diseases (NIAID) of the National Institutes of Health (NIH) following approval of animal safety protocols by the NIAID Animal Care and Use Committee.

Histopathology, immunohistochemistry, and digital microscopy. NBF-fixed mouse lungs were processed for histopathology and immunohistochemistry as previously described (15). Hematoxylin and eosin (H&E) stains were examined from two mice per virus group at 5 days p.i. Immunohistochemistry for influenza A virus antigen distribution used a goat polyclonal primary anti-influenza A virus (ab20841; Abcam, Cambridge, MA) and was completed on the same sets of tissues. All slides were scanned on an Aperio ScanScope XT system (Aperio, Vista, CA), enabling whole-slide analysis. Two pathologists reviewed these slides independently in a blinded fashion and then together in order to confirm consistent adherence to the scoring criteria. In order to compare degrees of lung pathology across the viruses, a lung pathology score of 0 to 3 (where 0 represented no pathology, and 3 represented severe pathology and the greatest degree of tissue involvement; see below) was given to each mouse by each pathologist, resulting in 4 pathology scores per virus. These scores were then averaged to obtain a single pathology score per virus. These scores are presented in Table 1. Lung sections were classified as mild influenza pneumonia (pathology score < 1.5), moderate influenza pneu-

monia (pathology score of 1.5 to 2.25), or severe influenza pneumonia (pathology score > 2.25).

Histologic descriptions for these 3 categories follow. Mild influenza pneumonia is defined as a pneumonic pattern characterized by a multifocal mild, predominantly lymphohistiocytic alveolitis and bronchiolitis, with low numbers of perivascular lymphocytes; and occasionally, a few bronchi had intraluminal inflammatory cells and/or necrotic debris. The extent of respiratory parenchyma involvement was up to 15%. Moderate influenza pneumonia is a pneumonic pattern characterized by a multifocal typically lymphohistiocytic and occasionally additionally neutrophilic, mild to moderate, occasionally severe alveolitis and bronchiolitis. Additionally, many mice had bronchitis, sometimes necrotizing. Perivascular lymphocytes were more prominent, and occasionally there was perivascular edema. The extent of respiratory parenchyma involvement was up to 25%. Severe influenza pneumonia is a pneumonic pattern characterized by a multifocal lymphohistiocytic or mixed (lymphohistiocytic and neutrophilic) moderate to severe alveolitis and bronchiolitis with occasional multifocal, marked fibrinous exudates. There was multifocal to nearly diffuse moderate to severe, frequently necrotizing, bronchitis. Perivascular lymphocytes and occasionally marked edema were also present. Up to 50% of respiratory parenchyma was involved.

Flow cytometric analyses. After euthanasia at 6 days p.i., the lungs were flushed of peripheral circulating cells by pushing 5 ml of PBS through the right ventricle of the heart. Lungs were then removed and placed in RPMI medium plus 10% fetal bovine serum (FBS) on ice. Lung tissues were minced with scalpels into 1- to 2-mm pieces and incubated with 1 U/ml collagenase D (Roche Applied Science, Indianapolis, IN) in RPMI for 30 min at 37°C. Minced pieces were pushed through 100-μm nylon mesh to create a single-cell suspension. Residual red blood cells were lysed with ACK lysis buffer (Sigma-Aldrich, St. Louis, MO). Cells were fixed with 2% paraformaldehyde (Sigma-Aldrich) at room temperature for 15 min in the dark. Approximately 2×10^6 cells were stained the following day with anti-CD16 (FcR block), CD4-phycoerythrin (PE), Ly6G-PE, I-A^d–fluorescein isothiocyanate (FITC), CD11c-FITC, SiglecF-Alexa Fluor 647, CD3-allophycocyanin (APC), CD45-peridinin chlorophyll protein (PerCP)-Cy5.5, CD11c-PE-Cy7, CD19-PE-Cy7, CD11b-V450, NKp46-V450, CD19-APC-Cy7, and CD8-APC-Cy7 (BD Biosciences, eBio, BioLegend, San Diego, CA) for 20 min at 4°C. Cells were analyzed using a BD FACSCanto II instrument (BD Biosciences) and FlowJo software (TreeStar, Ashland, OR).

Gene expression analyses. Tissues were collected at 1, 3, and 6 days p.i., and total RNA was isolated from whole mouse lungs of three individual mice in each group by homogenization in 10% (wt/vol) Trizol (Invitrogen, Grand Island, NY), followed by chloroform extraction and isopropanol precipitation. RNA quality was assessed using a BioAnalyzer instrument (Agilent Technologies, Santa Clara CA). For expression microarray analysis, equal masses of RNA isolated from lungs of individual infected animals were compared to a pool of RNA isolated from lungs of mock-infected mice.

Gene expression profiling experiments were performed using Agilent mouse whole-genome 44K microarrays (Agilent Technologies, Santa Clara CA). Fluorescent probes were prepared using the Agilent Quick-Amp labeling kit according to the manufacturer's instructions. Each RNA sample (three biological replicates per virus per time point) was labeled and hybridized to individual arrays. Spot quantitation was performed using Agilent's Feature Extractor software program, and all data were then entered into a custom-designed database, SlimArray, and then uploaded into the program GeneData Analyst 8.1 (GeneData, San Francisco, CA). Data normalization was performed in GeneData Analyst using central tendency followed by relative normalization using pooled RNA from mock-infected mouse lung as a reference. Expression analysis and statistical analysis, including t test and analysis of variance (ANOVA), were performed using the TIGR MultiExperiment Viewer 4.9 (62) and Tibco Spotfire 6.5 (Tibco Spotfire, Boston, MA) software programs.

NHBE cell culture and infection. Normal human bronchial epithelial (NHBE) cell cultures were differentiated and cultured in 24-well plates as described previously (63). For *in vitro* viral infections, all viruses were grown in NHBE cells at a multiplicity of infection (MOI) of 1, and 12 wells of the NHBE cells were infected for each virus at each time point for viral titers and pathology. Prior to infection the cells were washed two times with 300 μl PBS. Virus (1 MOI) in 100 μl PBS was added to each well, incubated for 1 h at 37°C, and then washed twice with 300 μl PBS, and then 100 μl PBS was added to each well and cells were incubated at 37°C in a humidified atmosphere with 5% CO_2. Cells and supernatants were harvested at 24, 48, 72, and 96 h after infection.

Statistical analysis. Mortality and the average number of days p.i. until death or endpoint euthanasia were analyzed by using ANOVA in the program GraphPad Prism version 5.0 (GraphPad Software Inc., La Jolla, CA); a P value of 0.05 or less was considered significant. Response variables that varied significantly by treatment group were further subjected to comparisons for all pairs by using the Tukey-Kramer test. Pairwise mean comparisons between inoculated and control groups were made using the Student t test.

SUPPLEMENTAL MATERIAL

Supplemental material for this article may be found at http://mbio.asm.org/lookup/suppl/doi:10.1128/mBio.02116-14/-/DCSupplemental.

Figure S1, PDF file, 0.2 MB.
Figure S2, PDF file, 0.1 MB.
Figure S3, PDF file, 0.3 MB.
Figure S4, PDF file, 0.2 MB.
Table S1, DOC file, 0.1 MB.

ACKNOWLEDGMENTS

REFERENCES

1. **Wright PF, Neumann G, Kawaoka Y.** 2007. Orthomyxoviruses, p 1691–1740. *In* Knipe DM, Howley PM (ed), Fields virology, vol 2, 5th ed. Lippincott Williams & Wilkins, Philadelphia, PA.

2. **Webster RG, Bean WJ, Gorman OT, Chambers TM, Kawaoka Y.** 1992. Evolution and ecology of influenza A viruses. Microbiol. Rev. **56:**152–179.

3. **Munster VJ, Baas C, Lexmond P, Waldenström J, Wallensten A, Fransson T, Rimmelzwaan GF, Beyer WE, Schutten M, Olsen B, Osterhaus AD, Fouchier RA.** 2007. Spatial, temporal, and species variation in prevalence of influenza A viruses in wild migratory birds. PLoS Pathog. **3:**e61. http://dx.doi.org/10.1371/journal.ppat.0030061.

4. **Dugan VG, Chen R, Spiro DJ, Sengamalay N, Zaborsky J, Ghedin E, Nolting J, Swayne DE, Runstadler JA, Happ GM, Senne DA, Wang R, Slemons RD, Holmes EC, Taubenberger JK.** 2008. The evolutionary genetics and emergence of avian influenza viruses in wild birds. PLoS Pathog. **4:**e1000076. http://dx.doi.org/10.1371/journal.ppat.1000076.

5. **Taubenberger JK, Kash JC.** 2010. Influenza virus evolution, host adaptation, and pandemic formation. Cell Host Microbe **7:**440–451. http://dx.doi.org/10.1016/j.chom.2010.05.009.

6. **Parrish CR, Holmes EC, Morens DM, Park EC, Burke DS, Calisher CH, Laughlin CA, Saif LJ, Daszak P.** 2008. Cross-species virus transmission and the emergence of new epidemic diseases. Microbiol. Mol. Biol. Rev. **72:**457–470. http://dx.doi.org/10.1128/MMBR.00004-08.

7. **Malik Peiris JS.** 2009. Avian influenza viruses in humans. Rev. Sci. Tech. **28:**161–173.

8. **Morens DM, Taubenberger JK, Fauci AS.** 2013. H7N9 avian influenza A virus and the perpetual challenge of potential human pandemicity. mBio **4(4):**e00445-13. http://dx.doi.org/10.1128/mBio.00445-13.

9. **Morens DM, Subbarao K, Taubenberger JK.** 2012. Engineering H5N1

avian influenza viruses to study human adaptation. Nature **486:**335–340. http://dx.doi.org/10.1038/nature11170.

10. **Wei SH, Yang JR, Wu HS, Chang MC, Lin JS, Lin CY, Liu YL, Lo YC, Yang CH, Chuang JH, Lin MC, Chung WC, Liao CH, Lee MS, Huang WT, Chen PJ, Liu MT, Chang FY.** 2013. Human infection with avian influenza A H6N1 virus: an epidemiological analysis. Lancet Respir. Med. **1:**771–778. http://dx.doi.org/10.1016/S2213-2600(13)70221-2.

11. **Liu D, Shi W, Gao GF.** 2014. Poultry carrying H9N2 act as incubators for novel human avian influenza viruses. Lancet **383:**869. http://dx.doi.org/10.1016/S0140-6736(14)60386-X.

12. **To KK, Tsang AK, Chan JF, Cheng VC, Chen H, Yuen KY.** 2014. Emergence in China of human disease due to avian influenza A(H10N8)—cause for concern? J. Infect. **68:**205–215. http://dx.doi.org/10.1016/j.jinf.2013.12.014.

13. **Johnson NP, Mueller J.** 2002. Updating the accounts: global mortality of the 1918-1920 "Spanish" influenza pandemic. Bull. Hist. Med. **76:**105–115. http://dx.doi.org/10.1353/bhm.2002.0022.

14. **Taubenberger JK, Reid AH, Lourens RM, Wang R, Jin G, Fanning TG.** 2005. Characterization of the 1918 influenza virus polymerase genes. Nature **437:**889–893. http://dx.doi.org/10.1038/nature04230.

15. **Qi L, Davis AS, Jagger BW, Schwartzman LM, Dunham EJ, Kash JC, Taubenberger JK.** 2012. Analysis by single-gene reassortment demonstrates that the 1918 influenza virus is functionally compatible with a low-pathogenicity avian influenza virus in mice. J. Virol. **86:**9211–9220. http://dx.doi.org/10.1128/JVI.00887-12.

16. **Dunham EJ, Dugan VG, Kaser EK, Perkins SE, Brown IH, Holmes EC, Taubenberger JK.** 2009. Different evolutionary trajectories of European avian-like and classical swine H1N1 influenza A viruses. J. Virol. **83:**5485–5494. http://dx.doi.org/10.1128/JVI.02565-08.

17. **Rabadan R, Levine AJ, Robins H.** 2006. Comparison of avian and human influenza A viruses reveals a mutational bias on the viral genomes. J. Virol. **80:**11887–11891. http://dx.doi.org/10.1128/JVI.01414-06.

18. **Taubenberger JK, Kash JC.** 2011. Insights on influenza pathogenesis from the grave. Virus Res. **162:**2–7. http://dx.doi.org/10.1016/j.virusres.2011.09.003.

19. **Taubenberger JK, Baltimore D, Doherty PC, Markel H, Morens DM, Webster RG, Wilson IA.** 2012. Reconstruction of the 1918 influenza virus: unexpected rewards from the past. mBio **3:**e00201-12. http://dx.doi.org/10.1128/mBio.00201-12.

20. **Pappas C, Aguilar PV, Basler CF, Solórzano A, Zeng H, Perrone LA, Palese P, García-Sastre A, Katz JM, Tumpey TM.** 2008. Single gene reassortants identify a critical role for PB1, HA, and NA in the high virulence of the 1918 pandemic influenza virus. Proc. Natl. Acad. Sci. U. S. A. **105:**3064–3069. http://dx.doi.org/10.1073/pnas.0711815105.

21. **Kobasa D, Takada A, Shinya K, Hatta M, Halfmann P, Theriault S, Suzuki H, Nishimura H, Mitamura K, Sugaya N, Usui T, Murata T, Maeda Y, Watanabe S, Suresh M, Suzuki T, Suzuki Y, Feldmann H, Kawaoka Y.** 2004. Enhanced virulence of influenza A viruses with the haemagglutinin of the 1918 pandemic virus. Nature **431:**703–707. http://dx.doi.org/10.1038/nature02951.

22. **Qi L, Kash JC, Dugan VG, Jagger BW, Lau YF, Sheng ZM, Crouch EC, Hartshorn KL, Taubenberger JK.** 2011. The ability of pandemic influenza virus hemagglutinins to induce lower respiratory pathology is associated with decreased surfactant protein D binding. Virology **412:**426–434. http://dx.doi.org/10.1016/j.virol.2011.01.029.

23. **Kash JC, Tumpey TM, Proll SC, Carter V, Perwitasari O, Thomas MJ, Basler CF, Palese P, Taubenberger JK, García-Sastre A, Swayne DE, Katze MG.** 2006. Genomic analysis of increased host immune and cell death responses induced by 1918 influenza virus. Nature **443:**578–581. http://dx.doi.org/10.1038/nature05181.

24. **Taubenberger JK, Morens DM.** 2008. The pathology of influenza virus infections. Annu. Rev. Pathol. **3:**499–522. http://dx.doi.org/10.1146/annurev.pathmechdis.3.121806.154316.

25. **Tumpey TM, Basler CF, Aguilar PV, Zeng H, Solórzano A, Swayne DE, Cox NJ, Katz JM, Taubenberger JK, Palese P, García-Sastre A.** 2005. Characterization of the reconstructed 1918 Spanish influenza pandemic virus. Science **310:**77–80. http://dx.doi.org/10.1126/science.1119392.

26. **Kobasa D, Jones SM, Shinya K, Kash JC, Copps J, Ebihara H, Hatta Y, Kim JH, Halfmann P, Hatta M, Feldmann F, Alimonti JB, Fernando L, Li Y, Katze MG, Feldmann H, Kawaoka Y.** 2007. Aberrant innate immune response in lethal infection of macaques with the 1918 influenza virus. Nature **445:**319–323. http://dx.doi.org/10.1038/nature05495.

27. **Memoli MJ, Tumpey TM, Jagger BW, Dugan VG, Sheng ZM, Qi L, Kash JC, Taubenberger JK.** 2009. An early "classical" swine H1N1 influenza virus shows similar pathogenicity to the 1918 pandemic virus in ferrets and mice. Virology **393:**338–345. http://dx.doi.org/10.1016/j.virol.2009.08.021.

28. **Subbarao EK, London W, Murphy BR.** 1993. A single amino acid in the PB2 gene of influenza A virus is a determinant of host range. J. Virol. **67:**1761–1764.

29. **Almond JW.** 1977. A single gene determines the host range of influenza virus. Nature **270:**617–618. http://dx.doi.org/10.1038/270617a0.

30. **Shinya K, Hamm S, Hatta M, Ito H, Ito T, Kawaoka Y.** 2004. PB2 amino acid at position 627 affects replicative efficiency, but not cell tropism, of Hong Kong H5N1 influenza A viruses in mice. Virology **320:**258–266. http://dx.doi.org/10.1016/j.virol.2003.11.030.

31. **Ma W, Lager KM, Li X, Janke BH, Mosier DA, Painter LE, Ulery ES, Ma J, Lekcharoensuk P, Webby RJ, Richt JA.** 2011. Pathogenicity of swine influenza viruses possessing an avian or swine-origin PB2 polymerase gene evaluated in mouse and pig models. Virology **410:**1–6. http://dx.doi.org/10.1016/j.virol.2010.10.027.

32. **Fornek JL, Gillim-Ross L, Santos C, Carter V, Ward JM, Cheng LI, Proll S, Katze MG, Subbarao K.** 2009. A single-amino-acid substitution in a polymerase protein of an H5N1 influenza virus is associated with systemic infection and impaired T-cell activation in mice. J. Virol. **83:**11102–11115. http://dx.doi.org/10.1128/JVI.00994-09.

33. **Gao R, Cao B, Hu Y, Feng Z, Wang D, Hu W, Chen J, Jie Z, Qiu H, Xu K, Xu X, Lu H, Zhu W, Gao Z, Xiang N, Shen Y, He Z, Gu Y, Zhang Z, Yang X, Zhao X, Zhou L, Li X, Zou S, Zhang Y, Yang L, Guo J, Dong J, Li Q, Dong L, Zhu Y, Bai T, Wang S, Hao P, Yang W, Han J, Yu H, Li D, Gao GF, Wu G, Wang Y, Yuan Z, Shu Y.** 2013. Human infection with a novel avian-origin influenza A (H7N9) virus. N. Engl. J. Med. **368:**1888–1897. http://dx.doi.org/10.1056/NEJMoa1304459.

34. **Hatta M, Gao P, Halfmann P, Kawaoka Y.** 2001. Molecular basis for high virulence of Hong Kong H5N1 influenza A viruses. Science **293:**1840–1842. http://dx.doi.org/10.1126/science.1062882.

35. **Hartshorn KL.** 2010. Role of surfactant protein A and D (SP-A and SP–D) in human antiviral host defense. Front. Biosci. (Schol. Ed.) **2:**527–546.

36. **Morens DM, Taubenberger JK.** 2011. Pandemic influenza: certain uncertainties. Rev. Med. Virol. **21:**262–284. http://dx.doi.org/10.1002/rmv.689.

37. **Jhung MA, Epperson S, Biggerstaff M, Allen D, Balish A, Barnes N, Beaudoin A, Berman L, Bidol S, Blanton L, Blythe D, Brammer L, D'Mello T, Danila R, Davis W, de Fijter S, Diorio M, Durand LO, Emery S, Fowler B, Garten R, Grant Y, Greenbaum A, Gubareva L, Havers F, Haupt T, House J, Ibrahim S, Jiang V, Jain S, Jernigan D, Kazmierczak J, Klimov A, Lindstrom S, Longenberger A, Lucas P, Lynfield R, McMorrow M, Moll M, Morin C, Ostroff S, Page SL, Park SY, Peters S, Quinn C, Reed C, Richards S, Scheftel J, Simwale O, Shu B, Soyemi K, Stauffer J, Steffens C, Su S, Torso L, Uyeki TM, Vetter S, Villanueva J, Wong KK, Shaw M, Bresee JS, Cox N, Finelli L.** 2013. Outbreak of variant influenza A(H3N2) virus in the United States. Clin. Infect. Dis. **57:**1703–1712. http://dx.doi.org/10.1093/cid/cit649.

38. **Taubenberger JK, Morens DM.** 2006, 1918. 1918 influenza: the mother of all pandemics. Emerg. Infect. Dis. **12:**15–22. http://dx.doi.org/10.3201/eid1209.050979.

39. **Kash JC, Xiao Y, Davis AS, Walters KA, Chertow DS, Easterbrook JD, Dunfee RL, Sandouk A, Jagger BW, Schwartzman LM, Kuestner RE, Wehr NB, Huffman K, Rosenthal RA, Ozinsky A, Levine RL, Doctrow SR, Taubenberger JK.** 2014. Treatment with the reactive oxygen species scavenger EUK-207 reduces lung damage and increases survival during 1918 influenza virus infection in mice. Free Radic. Biol. Med. **67:**235–247. http://dx.doi.org/10.1016/j.freeradbiomed.2013.10.014.

40. **Perrone LA, Plowden JK, García-Sastre A, Katz JM, Tumpey TM.** 2008. H5N1 and 1918 pandemic influenza virus infection results in early and excessive infiltration of macrophages and neutrophils in the lungs of mice. PLoS Pathog. **4:**e1000115. http://dx.doi.org/10.1371/journal.ppat.1000115.

41. **Tumpey TM, Szretter KJ, Van Hoeven N, Katz JM, Kochs G, Haller O, García-Sastre A, Staeheli P.** 2007. The Mx1 gene protects mice against the pandemic 1918 and highly lethal human H5N1 influenza viruses. J. Virol. **81:**10818–10821. http://dx.doi.org/10.1128/JVI.01116-07.

42. **Geiss GK, Salvatore M, Tumpey TM, Carter VS, Wang X, Basler CF, Taubenberger JK, Bumgarner RE, Palese P, Katze MG, García-Sastre A.** 2002. Cellular transcriptional profiling in influenza A virus-infected lung epithelial cells: the role of the nonstructural NS1 protein in the evasion of

the host innate defense and its potential contribution to pandemic influenza. Proc. Natl. Acad. Sci. U. S. A. **99:**10736–10741. http://dx.doi.org/10.1073/pnas.112338099.

43. **Sheng ZM, Chertow DS, Ambroggio X, McCall S, Przygodzki RM, Cunningham RE, Maximova OA, Kash JC, Morens DM, Taubenberger JK.** 2011. Autopsy series of 68 cases dying before and during the 1918 influenza pandemic peak. Proc. Natl. Acad. Sci. U. S. A. **108:**16416–16421. http://dx.doi.org/10.1073/pnas.1111179108.

44. **Xiao YL, Kash JC, Beres SB, Sheng ZM, Musser JM, Taubenberger JK.** 2013. High-throughput RNA sequencing of a formalin-fixed, paraffin-embedded autopsy lung tissue sample from the 1918 influenza pandemic. J. Pathol. **229:**535–545. http://dx.doi.org/10.1002/path.4145.

45. **WHO.** 28 February 2014. Human infections with avian influenza A(H7N9) virus. WHO, Geneva, Switzerland.

46. **Liu Q, Lu L, Sun Z, Chen GW, Wen Y, Jiang S.** 2013. Genomic signature and protein sequence analysis of a novel influenza A (H7N9) virus that causes an outbreak in humans in China. Microbes Infect. **15:**432–439. http://dx.doi.org/10.1016/j.micinf.2013.04.004.

47. **Chen Y, Liang W, Yang S, Wu N, Gao H, Sheng J, Yao H, Wo J, Fang Q, Cui D, Li Y, Yao X, Zhang Y, Wu H, Zheng S, Diao H, Xia S, Zhang Y, Chan KH, Tsoi HW, Teng JL, Song W, Wang P, Lau SY, Zheng M, Chan JF, To KK, Chen H, Li L.** 2013. Human infections with the emerging avian influenza A H7N9 virus from wet market poultry: clinical analysis and characterisation of viral genome. Lancet **381:**1916–1925. http://dx.doi.org/10.1016/S0140-6736(13)60903-4.

48. **Gabriel G, Dauber B, Wolff T, Planz O, Klenk HD, Stech J.** 2005. The viral polymerase mediates adaptation of an avian influenza virus to a mammalian host. Proc. Natl. Acad. Sci. U. S. A. **102:**18590–18595. http://dx.doi.org/10.1073/pnas.0507415102.

49. **Fouchier RA, Schneeberger PM, Rozendaal FW, Broekman JM, Kemink SA, Munster V, Kuiken T, Rimmelzwaan GF, Schutten M, Van Doornum GJ, Koch G, Bosman A, Koopmans M, Osterhaus AD.** 2004. Avian influenza A virus (H7N7) associated with human conjunctivitis and a fatal case of acute respiratory distress syndrome. Proc. Natl. Acad. Sci. U. S. A. **101:**1356–1361. http://dx.doi.org/10.1073/pnas.0308352100.

50. **Chen H, Yuan H, Gao R, Zhang J, Wang D, Xiong Y, Fan G, Yang F, Li X, Zhou J, Zou S, Yang L, Chen T, Dong L, Bo H, Zhao X, Zhang Y, Lan Y, Bai T, Dong J, Li Q, Wang S, Li H, Gong T, Shi Y, Ni X, Li J, Fan J, Wu J, Zhou X, Hu M, Wan J, Yang W, Li D, Wu G, Feng Z, Gao GF, Wang Y, Jin Q, Liu M, Shu Y.** 2014. Clinical and epidemiological characteristics of a fatal case of avian influenza A H10N8 virus infection: a descriptive study. Lancet **383:**714–721. http://dx.doi.org/10.1016/S0140-6736(14)60111-2.

51. **Klingeborn B, Englund L, Rott R, Juntti N, Rockborn G.** 1985. An avian influenza A virus killing a mammalian species—the mink. Brief report. Arch. Virol. **86:**347–351. http://dx.doi.org/10.1007/BF01309839.

52. **Zohari S, Metreveli G, Kiss I, Belák S, Berg M.** 2010. Full genome comparison and characterization of avian H10 viruses with different pathogenicity in mink (Mustela vison) reveals genetic and functional differences in the non-structural gene. Virol. J. **7:**145. http://dx.doi.org/10.1186/1743-422X-7-145.

53. **Wang G, Deng G, Shi J, Luo W, Zhang G, Zhang Q, Liu L, Jiang Y, Li C, Sriwilaijaroen N, Hiramatsu H, Suzuki Y, Kawaoka Y, Chen H.** 2014. H6 influenza viruses pose a potential threat to human health. J. Virol. **88:**3953–3964. http://dx.doi.org/10.1128/JVI.03292-13.

54. **Gillim-Ross L, Santos C, Chen Z, Aspelund A, Yang CF, Ye D, Jin H, Kemble G, Subbarao K.** 2008. Avian influenza h6 viruses productively infect and cause illness in mice and ferrets. J. Virol. **82:**10854–10863. http://dx.doi.org/10.1128/JVI.01206-08.

55. **Nam JH, Kim EH, Song D, Choi YK, Kim JK, Poo H.** 2011. Emergence of mammalian species-infectious and -pathogenic avian influenza H6N5 virus with no evidence of adaptation. J. Virol. **85:**13271–13277. http://dx.doi.org/10.1128/JVI.05038-11.

56. **Koçer ZA, Krauss S, Stallknecht DE, Rehg JE, Webster RG.** 2012. The potential of avian H1N1 influenza A viruses to replicate and cause disease in mammalian models. PLoS One **7:**e41609. http://dx.doi.org/10.1371/journal.pone.0041609.

57. **Bogs J, Kalthoff D, Veits J, Pavlova S, Schwemmle M, Mänz B, Mettenleiter TC, Stech J.** 2011. Reversion of PB2-627E to -627K during replication of an H5N1 clade 2.2 virus in mammalian hosts depends on the origin of the nucleoprotein. J. Virol. **85:**10691–10698. http://dx.doi.org/10.1128/JVI.00786-11.

58. **Krauss S, Walker D, Pryor SP, Niles L, Chenghong L, Hinshaw VS, Webster RG.** 2004. Influenza A viruses of migrating wild aquatic birds in North America. Vector Borne Zoonotic Dis. **4:**177–189. http://dx.doi.org/10.1089/1530366042162452.

59. **Watanabe T, Zhong G, Russell CA, Nakajima N, Hatta M, Hanson A, McBride R, Burke DF, Takahashi K, Fukuyama S, Tomita Y, Maher EA, Watanabe S, Imai M, Neumann G, Hasegawa H, Paulson JC, Smith DJ, Kawaoka Y.** 2014. Circulating avian influenza viruses closely related to the 1918 virus have pandemic potential. Cell Host Microbe **15:**692–705. http://dx.doi.org/10.1016/j.chom.2014.05.006.

60. **Yewdell JW.** 2013. To dream the impossible dream: universal influenza vaccination. Curr. Opin. Virol. **3:**316–321. http://dx.doi.org/10.1016/j.coviro.2013.05.008.

61. **Reed LJ, Muench H.** 1938. A simple method of estimating fifty percent endpoints. Am. J. Hyg. **27:**493–497.

62. **Saeed AI, Sharov V, White J, Li J, Liang W, Bhagabati N, Braisted J, Klapa M, Currier T, Thiagarajan M, Sturn A, Snuffin M, Rezantsev A, Popov D, Ryltsov A, Kostukovich E, Borisovsky I, Liu Z, Vinsavich A, Trush V, Quackenbush J.** 2003. TM4: a free, open-source system for microarray data management and analysis. Biotechniques **34:**374–378.

63. **Martinez-Anton A, Sokolowska M, Kern S, Davis AS, Alsaaty S, Taubenberger JK, Sun J, Cai R, Danner RL, Eberlein M, Logun C, Shelhamer JH.** 2013. Changes in microRNA and mRNA expression with differentiation of human bronchial epithelial cells. Am. J. Respir. Cell Mol. Biol. **49:**384–395. http://dx.doi.org/10.1165/rcmb.2012-0368OC.